Dynamic control of urban sewer systems to reduce combined sewer overflows and their adverse impacts

Upaka Rathnayake[1*] and A.H.M. Faisal Anwar[2]

[1]Department of Civil Engineering, Faculty of Engineering, Sri Lanka Institute of Information Technology, New Kandy Road, Malabe, Sri Lanka

[2] Department of Civil Engineering, Curtin University, GPO Box U1987, Perth WA 6845, Australia

[*]Corresponding email: upakasanjeewa@gmail.com / upaka.r@sliit.lk

Highlights

- Optimal control model is developed to control the existing combined sewer networks.
- Multi-objective optimization techniques are applied to the control model to minimize the pollution load to receiving water and the cost of wastewater treatment together with cost of pump operation.
- Spatial and temporal variations of flow and water qualities in stormwater runoff are considered to the model.
- The model can control the gates dynamically with respect to the time, based on the feedback from the control settings of the previous time-step.

Abstract

Sewer network planners use control algorithms, based on optimization techniques, to control urban wastewater systems. These control algorithms have been used to ease the stress on the sewer networks and then, to reduce or to minimize the combined sewer overflows (CSOs). CSOs are not only risking human health but also adversely affecting the aquatic lives. Therefore, many cities try to avoid CSOs. However, this cannot be done to the perfect level due to the capacity limitations of the existing combined sewer networks. In addition, climate variabilities have caused unpredictable precipitation increments and therefore, the control is extremely difficult. Therefore, considering the spatial and temporal variations of runoffs and qualities of stormwater generated from the precipitation, an enhanced optimal control algorithm is illustrated in this paper to control the existing combined sewer networks. Minimizing the pollution load to the receiving water and minimizing the cost of wastewater treatment and pump operation are the two objective functions in the developed optimization algorithm. The algorithm was then successfully applied to a real-world combined sewer network in Liverpool, United Kingdom. Results reveal that the developed optimal control model is capable of handling the dynamic control settings of combined sewer system to minimize the two objective functions simultaneously. With a little computational appreciation, the developed optimal control model can be well-used in the real-time control of combined sewer networks.

Keywords: Combined sewer overflows (CSOs), dynamic control, evolutionary algorithms, multi-objective optimization, orifice gate openings, pumping cost

1. Introduction

In many countries, the existing sewer networks are not designed to handle the collective stormwater and wastewater during the stormy periods (Zhao *et al.,* 2017*)*. Because of this capacity limitation, combined sewer overflows (CSOs) occur. Moreover, on-going climate variability and climate changes may cause intensified precipitation events in some areas which may also lead to frequent CSOs (Tavakol-Davani *et al.,* 2016; Dirckx *et al.,* 2017; Jean *et al.,* 2018; Zhang *et al.,* 2018a). Though, CSOs sometimes prevent flooding in important places (Zhao *et al.,* 2017) but it can bring significant environmental risk if they are not properly controlled (Jalliffier-Verne *et al.,* 2016; Madoux-Humery *et al.,* 2016; Brokamp *et al.,* 2017). The receiving water bodies are in danger due to sudden accumulation of pollution loads from CSOs (Zhang *et al.,* 2018b; Schertzinger *et al.,* 2019; Soriano and Rubió, 2019). Many researchers conducted detailed research on identifying the various pollutants in CSOs, impact of CSOs on ecosystem and drinking water qualities (Gasperi *et al.,* 2012; Jalliffier-Verne *et al.,* 2016; García *et al.,* 2017; Hermoso *et al.,* 2018; Wei *et al.,* 2019). García *et al.,* (2017) have experimentally obtained the pollutographs for two cities in Spain along the lines of CSOs. Rathnayake (2013) also derived pollutographs for various water quality constituents considering spatial and temporal variations. Again, the CSOs can cause severe urban flooding (Meneses *et al.,* 2018) at unexpected locations and reduce the wastewater treatment plants' efficiency (Zhang *et al.,* 2018b). Therefore, minimizing CSOs in urban areas is an important task for many municipal councils. These may be done by using structural or non-structural measures. The physical constructions developed to reduce the CSOs are the structural measures in controlling CSOs (for example, underground tunnels to store combined sewer flows in stormy days). However, Non-structural measures do not involve any physical constructions but they involve the usage of knowledge and experiences to develop various policies and control approaches to reduce the CSOs in existing sewer networks. The financial capabilities and disturbances to the habitants have limited the structural measures in minimizing the CSOs (Zhang *et al.,* 2018a). Thus, non-structural measures are given a higher priority in today's world. Therefore, non-structural measures, including control algorithms based on optimization theories, are becoming popular (Zimmer *et al.,* 2015 & 2018). Nevertheless, structural measures are still used when the space and financial capacities are permitted (Nasri and Haynes, 2015).

Even though, the non-structural measures are used to overcome the issues from CSOs, multiple interactions in various sub-systems such as, catchments, sewer systems, wastewater treatment plant and receiving water bodies make the control of urban wastewater system a greater challenge (Saagi *et al.,* 2016 & 2018). In addition, the dynamic behavior of flow and wastewater quality in sewer systems make the scenario more complex (Rathnayake and Tanyimboh, 2015). Therefore, a holistic solution for the optimal control of combined sewer system is still to be tabled.

Many researchers showcased the usage of green infrastructure (GI) as a measure to reduce the CSOs (Lucas and Sample, 2015; Sørup *et al.,* 2016; Tao *et al.,* 2017; Talebi and Pitt, 2019). Green infrastructure is an approach to balance the natural water cycle using engineered or non-engineered techniques of water management. Some other researchers have introduced model predictive control (MPC) approaches to minimize CSOs (Joseph-Duran *et al.,* 2015; Zhao *et al.,* 2017; Snodgrass *et al.,* 2018). Zimmer *et al.,* (2015) presented an MPC model to reduce the CSOs for a deep-tunnel sewer system. They have further extended their work (Zimmer *et al.,* 2018) to explore the efficiency and effectiveness of different MPC approaches.

Storage tanks in combined sewer systems are utilized properly as another solution to CSOs. The overall idea of this method is to reduce the CSOs volume flow rates. Therefore, these control models are based on the volumetric measures. Models based on storage tanks have been applied as case studies in many places (Ryu *et al.,* 2015; Hermoso *et al.,* 2018; Georgaki *et al.,* 2018; Wang and Guo, 2018; Zhang *et al.,* 2018a; Zhang *et al.,* 2018b). These studies include the optimal sizing and optimal locating of storage tanks (Hermoso *et al.,* 2018).

Real time control (RTC) plays a major role in sewer network control. The control algorithms continuously get the feedback from the sewer system and adjust the settings accordingly. However, this is not easily applicable for all combined sewer systems, due to the logistical issues. Nevertheless, many researchers tried to implement RTC strategies to combined sewer systems as a holistic solution for CSOs (Enterm *et al.,* 1998; Dirckx *et al.,* 2017; Mahmoodian *et al.,* 2017; Meneses *et al.,* 2018; Congcong *et al.,* 2019). However, some of these simplified RTC systems can be found in many places to measure the water quality constituents which may include Graz in Austria (Hofer *et al.,* 2018), Copenhagen in Denmark (Vezzaro *et al.,* 2014), Lodz in Poland (Brzezińska *et al.,* 2016), Trondheim (Weinteich *et al.,* 1997) and Fredrikstad (Nie *et al.,* 2009) in Norway and Wilhelmshaven (Seggelke *et al.,* 2013) and Odenthal (Erbe *et al.,* 2002) in Germany. These RTC models in sewer systems are simple but fast in computation (Mahmoodian *et al.,* 2017). But dynamic control based on receiving water qualities and minimizing CSOs is yet to be presented. Nevertheless, optimization techniques including multi-objective optimization are widely used in these control algorithms (Mauricio-Iglesias *et al.,* 2015; Morales *et al.,* 2015; Morales, 2016; Ogidan *et al.,* 2016). Therefore, there is a need for a holistic approach to minimize the CSOs and maximize the receiving water qualities considering the dynamic spatial and temporal behaviors of the sewer systems and its attributes. This paper presents a novel dynamic control algorithm based on the pollution control in receiving water due to CSOs and overall treatment and pumping cost of the sewer network. The control algorithm is based on the multi-objective optimization function to minimize both pollution load to receiving water and overall cost in sewer system simultaneously. In addition, it is capable of presenting dynamic control strategies based on the feedback, unlike most other rule-based control strategies. The temporal and spatial variation of pollutants in stormwater runoff is also highly important in finding the pollution load to the receiving water from various locations (Anne-Sophie *et al.,* 2015; Müller *et al.,* 2017). Therefore, the presented method is capable of handling both spatial and temporal distributions of stromwater flow rates and also the various pollution concentrations in stormwater. The developed novel dynamic control algorithm was successfully tested to the real world combined sewer network and promising results are presented.

2. Hydraulics of the storage tanks in sewer networks

Storage tanks in sewer networks play an important role in minimizing possible CSOs. They store wastewater during the stressed (stormy) periods and release back to the sewer network in non-stressed (dry) periods. The storage tanks are very common in combined sewer networks and can be categorized into on-line storage tanks or off-line storage tanks (Read and Vickridge, 1997; Read 2004). The storage tank category is mainly selected based on the surrounding land areas and land uses of the sewer networks. If the land area is crowded or highly valuable, the sewer network planners can decide to have the storage tank at a faraway location where the land area is not much valuable. This process requires additional hydraulic components such as pumps to have two directional flows. If surrounding land area is not so costly, the storage tanks can be placed nearer to the sewer system, and thus the control is easy and it may not require a pump. Therefore, a complex larger sewer network may have both features of on-line storage tanks and/or off-line storage tanks.

On-line storage tanks are attached to the CSO chambers. The schematic diagrams of on-line and off-line storage tanks are shown in Figure. 1. The on-line storage tanks start to fill (q_s) when the inflow ($I_{i,t}$) is more than the maximum allowable through flow ($Q_{i,t}$) to the sewer network (Figure 1a). A throttle is usually used to control the discharge from the on-line storage tank. When the water level in the storage tank reaches to the maximum, the flow to the storage tank from sewer chamber is blocked. Therefore, the system allows the sewer chamber to have overflows ($O_{i,t}$). However, when the water level in sewer chamber reduces to a controllable level, the bottom orifice combining storage tank and sewer chamber is opened and the stored flow is easily transferred back to the sewer chamber.

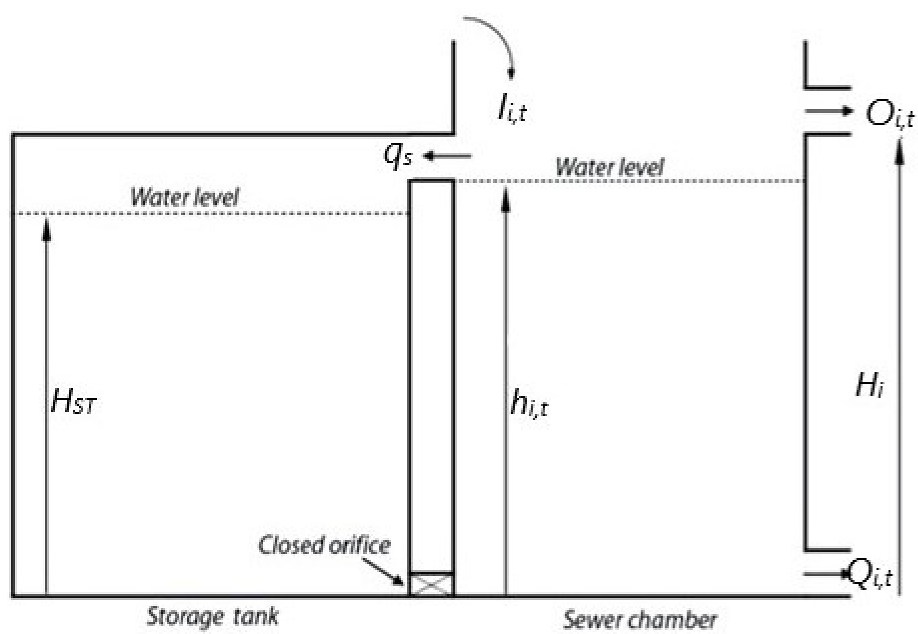

q_s – flow to the storage tank from sewer chamber

H_{ST} – water level of the storage tank

$h_{i,t}$ – water level in the sewer chamber

H_i – spill level of the sewer chamber

$I_{i,t}$ – catchment inflow to i^{th} interceptor node

$O_{i,t}$ – flow from i^{th} sewer chamber to i^{th} interceptor node

$Q_{i,t}$ – combined sewer overflow discharge at i^{th} interceptor node

(a)

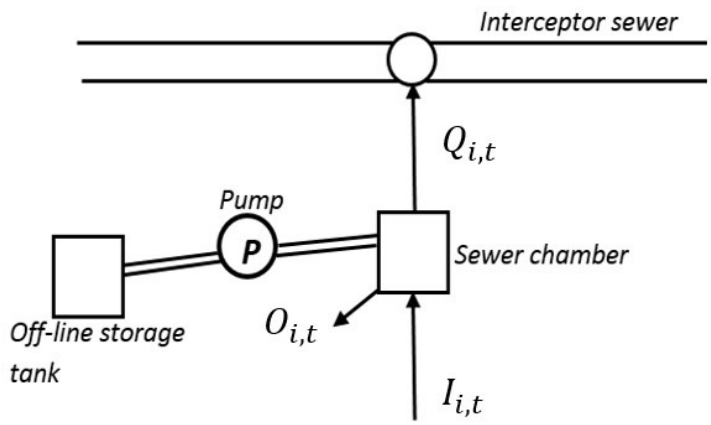

(b)

Figure 1. Schematic diagram of sewer chamber with (a) on-line storage tank and (b) off-line storage tank

Figure 1b shows the schematic diagram of the off-line storage tank in the combined sewer systems. Unlike the on-line storage tanks, the off-line storage tanks are physically separated from CSO chambers. The off-line storage tanks are placed far away from the sewer chambers. When the land area around sewer chambers are highly valuable, the designers move the on-line storage tanks to off-line storage tanks. Therefore, storage tanks in sewer system in rural areas may be preferable than the urban areas.

The flow is diverted to the off-line tank from the sewer chamber during the stormy seasons. This can either be via gravity fed pipes or pumped pipes. During unstressed periods the stored wastewater can be released back to the sewer chamber. However, the releasing of wastewater must be via pumped pipes if wastewater was diverted via gravity fed pipes or vice versa. Therefore, the off-line storage tank always comes with a hydraulic pump, which add an additional cost to the operation. But the extended pipeline (away from the sewer chamber) in off-line storage tank also gives an additional storage facility during the stormy period.

3. Mathematical formulation for the optimization problem

This section presents a development of an algorithm to control the combined sewer systems dynamically. The dynamic control is based on the feedback from each time-steps by solving the following multi-objective optimization algorithm. The developed algorithm considers two objective functions which are time, flow and water quality dependent.

3.1 Objective functions

The first objective function (F_1) is formulated to minimize the pollution load discharges to the natural water from the CSOs at each time-step. The mathematical expression of the first objective function is given in the Equation 1.

$$F_1 = Minimize \sum_{i=1}^{n} P_i \tag{1}$$

where P_i is the pollution load discharged from i^{th} sewer chamber at a given time-step and n is the number of CSOs or number of sewer chambers. P_i is calculated using the effluent quality index (*EQI*) defined to each CSO. *EQI* is a single index to measure the pollution load. It integrates several pollutants together including the concentrations of total suspended solid (*TSS*), biochemical oxygen demand (*BOD*), chemical oxygen demand (*COD*), nitrates and nitrites (NO_X), total Kjedahl nitrogen (*TKN*) and total phosphorus (*TP*). Equation 2 gives the mathematical expression for the *EQI*.

$$P_i = EQI_i = \frac{1}{1000\left(t_f - t_0\right)} \int_{t_0}^{t_f} \left(2C_{TSS} + C_{COD} + 2C_{BOD} + 20C_{NOX} + 20C_{TKN} + 100C_{TP}\right) Q_e\left(t\right) dt \qquad (2)$$

where $Q_e(t)$, t_f and t_0 are the combined sewer overflow rate, final and initial time, respectively. C_{TSS}, C_{COD}, C_{NOX}, C_{BOD}, C_{TKN} and C_{TP} are the concentrations of total suspended solids, chemical oxygen demand, nitrates and nitrites, five-day biochemical oxygen demand, total Kjeldahl nitrogen and total phosphate, respectively and measured in milligram per liters (mg/L). Numerical values in front of the concentrations are the weightages used to integrate the different pollutants to build up the pollution load. More information on this effluent quality index can be found in Benedetti *et al.,* (2006), Kim *et al.,* (2009) and Rathnayake (2018).

The second objective function (F_2) is formulated to minimize the treatment plant cost and the operational cost of pumps in the sewer system at a given time-step. The mathematical behavior of the objective function is presented in Equation 3.

$$F_2 = Minimize\ (C_T + C_P) \qquad (3)$$

where C_T (€/year) is the wastewater treatment plant cost and the C_P (€/year) is the operational cost of pumps in sewer system. C_T and C_P are based on the wastewater flowrate. For example, for a particular system, the pump cost is calculated based on the wastewater volume, which is pumped from the hydraulic pump. Cost of treatment plant can be expressed according to the Equation 4.

$$C_T = \begin{cases} 1642353 \times q_T^{0.659}, & q_T \leq 3q_{dry} \\ 1891.154 \times q_{dry}^{0.659} + 7.84 \times q_T - 3.38 \times q_{dry} + 7584, & 6q_{dry} \geq q_T \geq 3q_{dry} \\ 1891.154 \times q_{dry}^{0.659} + 3.38 \times q_{dry} + 7584, & 6q_{dry} \leq q_T \end{cases} \quad (4)$$

where q_T (m^3/s) and q_{Tdry} (m^3/s) are the treated wastewater volume flowrate and the dry weather flowrate, respectively. More information about this treatment plant cost function can be found in Rathnayake and Tanyimboh (2015) and Rathnayake (2013). The above presented treatment cost function looks at the total operational cost of wastewater treatment plant including, wastewater treatment cost, personal cost, energy cost, maintenance cost, etc. In addition, the treatment cost formula can be modified time-to-time using a simple coefficient based on the considered country's economy.

The pump operational cost (C_P) is formulated as a function of pumped wastewater volume flow rate (Q_P) given in Equation 5. The equation developed is based on the power required to pump the wastewater to the required head and it is a function of the pumped wastewater volume flow rate.

$$C_P = K \frac{\rho g H_P}{\eta_{pump} \eta_{motor} t_P} Q_P \quad (5)$$

where K, ρ, g, H_P, η_{pump}, η_{motor} and t_P are the cost for unit power in electricity, density of wastewater, gravitational acceleration, head given to the wastewater by the pump, efficiency of the pump, efficiency of the motor and pump operation time, respectively. More information on the development of this generic pump operational cost can be found in Rathnayake (2018).

3.2 Constraints

The above stated two objective functions (F_1 and F_2) are under a set of constraints. In other words, the solutions of these two objective functions must be limited to the given set of constraints. The sewer system hydraulically satisfies the continuity equation. Figure 2 shows the schematics of the node in the sewer network. Referring to the Figure 2, the continuity equations can be illustrated as shown in Equations 6 - 8.

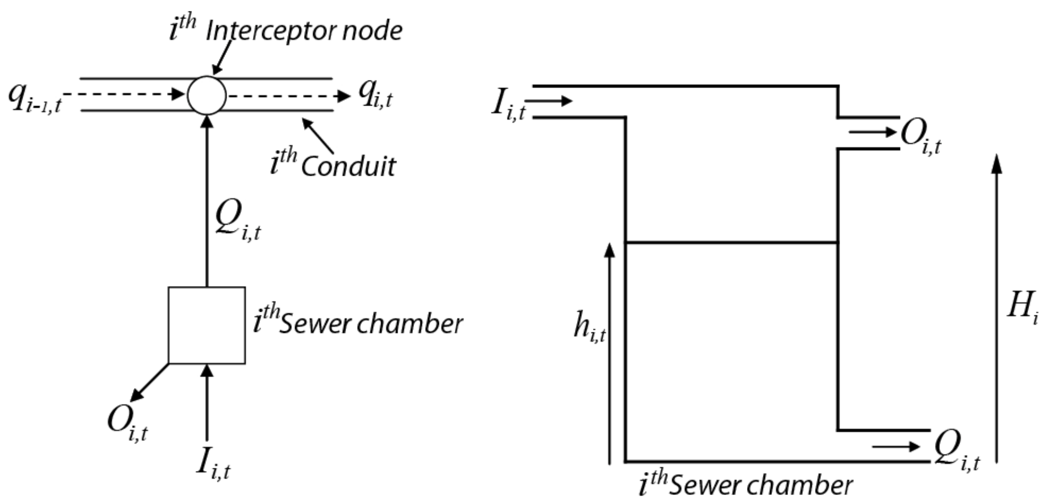

$I_{i,t}$ – catchment inflow to i^{th} interceptor node

$Q_{i,t}$ – combined sewer overflow discharge at i^{th} interceptor node

$q_{i,t}$ – through flow in interceptor sewer at i^{th} node

$O_{i,t}$ – flow from i^{th} sewer chamber to i^{th} interceptor node

$h_{i,t}$ – water level in the sewer chamber

H_i – spill level of the sewer chamber

Figure 2 Schematic diagram of combined sewer chamber

$$Q_{i,t} + q_{i-1,t} - q_{i,t} = 0 \tag{6}$$

$$A_C \frac{\Delta h_{i,t}}{\Delta t} = I_{i,t} - Q_{i,t}\,; \qquad h_{i,t} < H_i \tag{7}$$

$$A_C \frac{\Delta h_{i,t}}{\Delta t} = I_{i,t} - Q_{i,t} - O_{i,t}\,; \qquad h_{i,t} > H_i \tag{8}$$

where A_C is the surface area of the sewer chamber. In addition, the sewer system is under the capacity constraints. They are introduced to satisfy the non-silting and non-scouring flow rates (velocities) in sewer network. These capacity constraints are given in Equation 9.

$$0 \leq q_{i,t} \leq q_{max,i} \tag{9}$$

where $q_{i,t}$ and $q_{max,i}$ are the flow rates inside the i^{th} sewer conduit at time *t* and the maximum allowable flow rate in i^{th} sewer conduit, respectively.

3.3 Solution technique for the optimization problem

Multi-objective optimization problems can be solved in various ways (Marler and Arora, 2004). Weighted global criterion method (Zhang and Shivpuri, 2009; Costa *et al.*, 2011; Zhao *et al.*, 2012), weighted sum method (Kim and de Weck, 2004; Marler and Arora, 2009; Wang *et al.*, 2018), Lexicographic method (Sun *et al.*, 1999; Jee *et al.*, 2007; Aghaei *et al.*, 2011), weighted min-max method (Wang *et al.*, 1996; Shimoda *et al.*, 1996; Singh, 2002), exponential weighted criterion (Carpinelli *et al.*, 2014 ; Kang *et al.*, 2014), weighted product method (Wang *et al.*, 2010), goal programming methods (Charnes and Cooper, 1977; Hu *et al.*, 2007), bounded objective function method (Abo-Sinna and Baky, 2007; Zheng *et al.*, 2011), physical programming methods (Qiu *et al.*, 2011; Yuan *et al.*, 2014) and generic algorithms (Grefenstette, 1986; Srinivas and Deb, 1994) are several methods in the literature to obtain solutions from multi-objective optimization problems. A genetic algorithm-based optimization solver was used to obtain the optimal solutions for the developed multi-objective optimization problem in this study. Despite the other available approaches, a genetic algorithm solver was selected due to the complexity of the optimization problem.

Genetic algorithms mimic the biological evolution in searching for the minimum or maximum solutions (Marler and Arora, 2004). They continuously update the population of solutions in each step. Crossover and mutation processes are introduced by most of the generic algorithms to produce new offspring (children) from the parent population. More information on the process of genetic algorithms can be found in Davis (1991).

Two objective functions given in Equations 1 and 3 were solved in the genetic algorithms' environment. However, these objective functions were treated independently without simplifying them to one objective function using relative weights. As it was explicitly stated in Equations 2, 4 and 5, the two objective functions vary with time and space. Therefore, the temporal and spatial variation of flow rates and concentrations of various water quality constituents are included. The parameters which are used to calculate the objective functions (F_1 and F_2) were directly obtained from the complete hydraulic simulations and water quality simulations of the sewer network. Therefore, the hydraulic simulations and water quality simulations were carried out for number of function evaluations (for example 10000 function evaluations) and more importantly, the full hydraulic simulations were carried out using Saint-Venant equations.

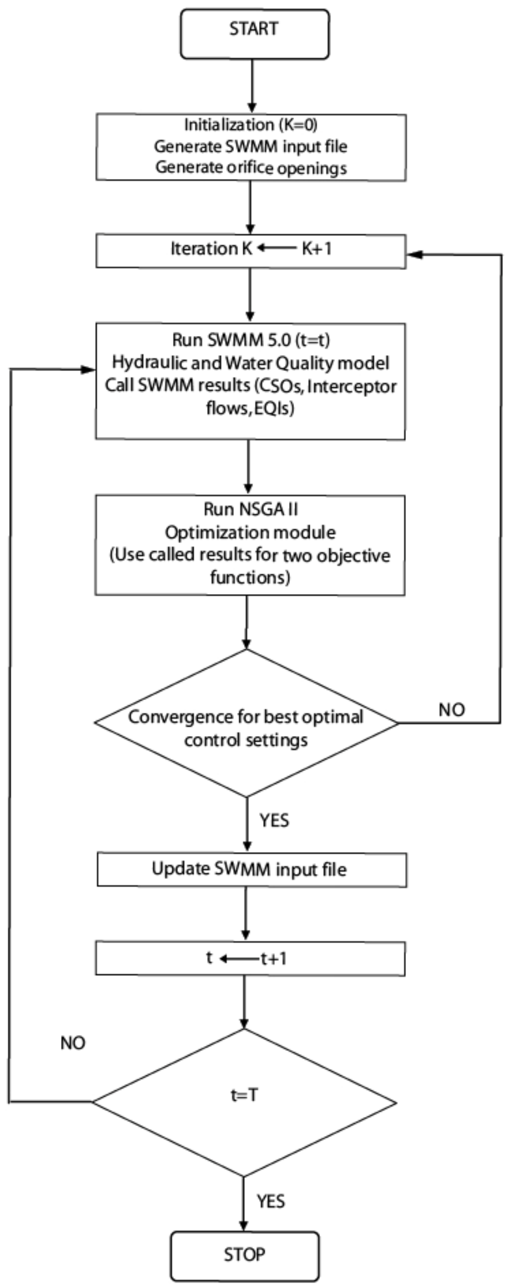

Figure 3 Flowchart to the solution algorithm for the developed multi-objective optimization problem

Hydraulic model, SWMM 5.0 (Rossman, 2009) and multi-objective optimization module, NSGA II (Deb *et al.*, 2002) were linked together to obtain the above stated parameters (inputs of the multi-objective optimization problem). SWMM 5.0 was developed by the U.S. Environmental Protection Agency (USEPA) and applied to many real-world examples all over the world (Berndtsson and Niemczynowicz, 1988; Rodriguez *et al.*, 2003; Maneta *et al.*, 2007; Leisenring and Moradkhani, 2012; Brunetti *et al.*, 2016). The model is capable of conducting simulations and analysis to stormwater networks and sewer network to satisfy the hydrological, hydraulics and water quality requirements. On the other hand, NSGA II optimization algorithm is extensively used in real-world optimization problems including water resource management issues (Alizadeh *et al.*, 2017; Bekele and Nicklow, 2007; Chang and Chang, 2009; Lei *et al.*, 2018; Naserizade *et al.*, 2018).

A set of orifices with gates placed in the CSO chambers were used to control the flow in the combined sewer system. Therefore, the decision variables of the developed multi-objective optimization problem are the gate openings of the orifices at different time-steps. The flowchart to the solution algorithm is presented in Figure 3. The gate openings in the orifices for the first time-step (0 – 15 minutes) were randomly generated in NSGA II. Then, a full hydraulic simulation including water quality of the wastewater was carried out inside the SWMM 5.0 hydraulic model. The results from the simulation were fed to the NSGA II optimization algorithm and the two objective functions (F_1 and F_2) were calculated accordingly. Then, the optimization algorithm was run to identify the optimal solutions. Depending on the sewer network controller, one optimal solution was selected from the Pareto optimal front and the control settings for that optimal solution were obtained. Those control settings (gate openings) were then, used as the input data for first time step in the hydraulic model for the second time-step (15 – 30 minutes) optimization process. The process was carried out for the whole storm period and control settings were obtained. Finally, sets of orifice gate openings were presented and these control settings can be used by the sewer network controllers.

4. Real world application

A real-world combined sewer network in Liverpool, United Kingdom was selected to test the developed dynamic control model. The interceptor sewer network (*around 3200 m long*) given by Thomas *et al.* (1999, 2000) and Thomas (2000) was further modified to incorporate the objective functions (F_1 and F_2). These modifications include an introduction of several storage tanks (both on-line and off-line) and a hydraulic pump (***P***) to the off-line storage tank (***T10***). More details about these modifications can be found in Rathnayake (2018). The schematic diagram for the modified interceptor sewer network is given in Figure 4.

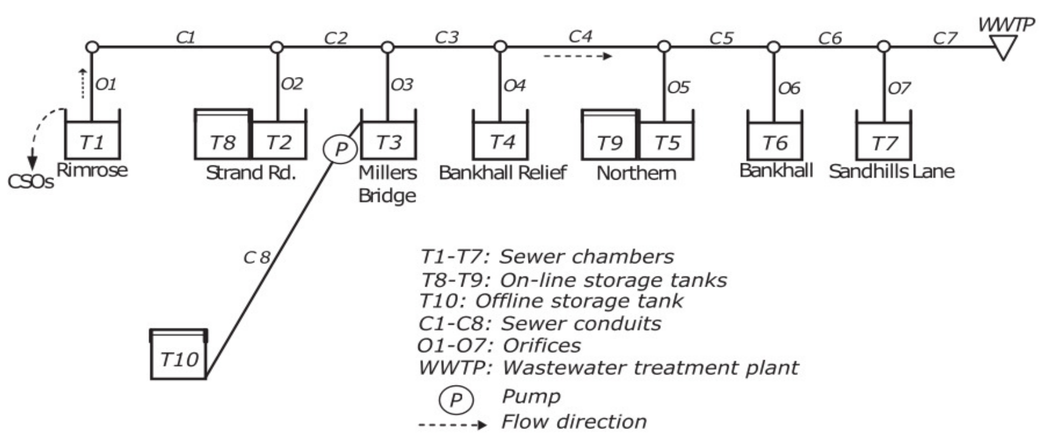

Figure 4 Schematic diagram of interceptor sewer

The on-line storage tanks (*T8* and *T9*) start to fill automatically when the wastewater level in the corresponding sewer chambers (*T2* and *T5*, respectively) reaches the maximum capacities. The on-line storage tanks stop the inflow wastewater, when they reach their maximum capacities. Therefore, the on-line storage tanks do not allow any CSOs. The stored wastewater can be released back to the sewer system at the lower stressed periods. The control settings of the off-line storage tank (*T10*) are slightly different from the on-line storage tanks. When the wastewater level reaches to the spill level of the sewer chamber (*T3*), the wastewater is pumped to the off-line storage tank. However, the pump stops its operations when the off-line storage tank reaches to the maximum capacity. However, the stored wastewater is released back to the sewer system in a less stressed period under the gravity. These control settings in the storage tanks and pump were done using the control rules of the hydraulic model.

The wastewater flows through the conduits (*C1* to *C7*) are constrained according to the Equation 9. The flows through *C1* to *C3* were kept at 3.26 m^3/s and those of *C4* to *C7* were kept at 7.72 m^3/s. More details about the dimensions of the sewer chambers and conduits can be found in Rathnayake (2013, 2018). *T10* off-line storage tank was placed 2 km away from the corresponding sewer chamber, *T3*. The elevation difference from *T3* to *T10* is 21 m and the chamber and the off-line storage tank are connected by 0.2 m diameter, 2000 m long conduit. Therefore, a pump (*P*) was introduced to allow the wastewater flow from *T3* sewer chamber to *T10* off-line storage tank. The pump automatically starts and pumps water from *T3* to *T10* when the wastewater level in *T3* reaches to its spill level (**6 m**). The pump automatically stops when the wastewater in the *T10* reaches to its maximum capacity and also if the wastewater level in *T3* sewer chamber reduces to an acceptable level (**4 m** level). These automated controls were coded inside the SWMM 5.0 hydraulic model using the pump control rules.

Stormwater inflows from seven different catchments were fed to the sewer chambers. The catchment names are listed at corresponding sewer chambers (Figure 4). They are Rimrose, Strand Road, Millers Bridge, Bankhall Relief, Northern, Bankhall and Sandhills Lane. Five different land-uses (residential, industrial, agricultural, mid urban and commercial) were assigned to these catchments. More details on the catchments and their land-uses can be found in Rathnayake (2013). Stormwater runoff includes runoff hydrographs from 2.5 hours storms for each catchment and pollutographs for the corresponding runoff hydrographs. *TSS*, *COD*, *BOD*, *TKN*, NO_X and *TP* pollutographs were fed to each sewer chamber from the corresponding catchments. Therefore, the sewer chambers have inputs of spatial and temporal variations of runoffs and six different pollutographs. In addition, the flow rates from dry weather flows and the corresponding concentrations of pollution constituents were fed. More information on these inputs to the sewer chambers can be found in Rathnayake (2013, 2018) and Rathnayake and Tanyimboh (2015).

Using the sewer flow dynamics in flow rates and wastewater qualities stated above, the developed multi-objective optimization algorithm was run to obtain the optimal solutions (F_1 and F_2). 10,000 function evaluations for one time-step (10,000 hydraulic and water quality simulations per one time-step) were carried out using the real coded NSGA II optimization algorithm. The gates introduced at sewer chambers were controlled according to the optimization algorithm based on the pollution load to the receiving water and the total cost of the system. Therefore, the gates of the sewer networks were controlled dynamically (with time and space); however, according to the solutions from the developed multi-objective optimization approach.

Real coded optimization algorithm generates solutions in real numbers. This is important in gate controls as gate openings can be any value in between the minimum (fully closed) and maximum (fully opened). Population sizes of 100 for 100 generations were chosen for the optimization process. The crossover probability was kept at 0.9 (Deb *et al.,* 2002); however, different mutation probabilities were tested while calibrating the algorithm. Several random seeds were used for random runs for each time-step to check the convergence of the optimization algorithm. The optimization algorithm was initially run for the first time-step (0-15 minutes) and then, two extreme solutions were selected for the further analysis. They were minimum cost solution and the minimum pollution load solution. The gate openings were obtained for these two solutions and fed to obtain the two optimal corresponding solutions for the next time step. Similarly, optimal control settings for the other time steps (15 minutes by 15 minutes) until the end of the storm were obtained for the two extreme solutions (minimum cost and minimum pollution load). These simulations were carried out in a personal computer (Intel® Core™ i3) which has 3.40 GHz and 4 GB RAM. The simulation times were about 10-50 minutes.

5. Results and discussion

Results and discussion section is divided into several subsections to illustrate the results in detail. It starts with the optimization results for the time-step (0-15 minutes) and identified two potential optimal solutions to proceed for the dynamic optimization process. Results of the overall robustness of the developed algorithm is then presented. Next, the optimal control settings of the gates are presented to illustrate the dynamic behavior of the control in the time axis. Finally, the hydraulic verification results are presented to verify the developed multi-objective optimization model in control of the combined sewer system.

As it was stated in the preceding paragraph, the optimization simulations were carried out for two different solutions; the minimum pollution load solution and the minimum cost solution until the end of the storm runoff. However, the optimization simulations were performed at 15 minutes time steps; thus, the control settings (gate openings) can be obtained in the intervals of 15 minutes until the end of storm. The simulations started at 0 – 15 minutes and then, proceeded for the next 15 minutes.

5.1 Optimization solutions for the first time-steps (0-15 minutes)

Pareto optimal front for the first time-step for 0-15 minutes is shown in Figure 5. The shape of the Pareto optimal front clearly presents minimizing behavior of the two objective functions. Two extreme solutions (minimum pollution load and minimum cost) were selected for the optimization process for the 15-30 minutes time-step. These two extreme solutions are shown as MP_{t1} (minimum pollution load solution at first time step) and MC_{t1} (minimum cost solution at first time step) in Figure 5.

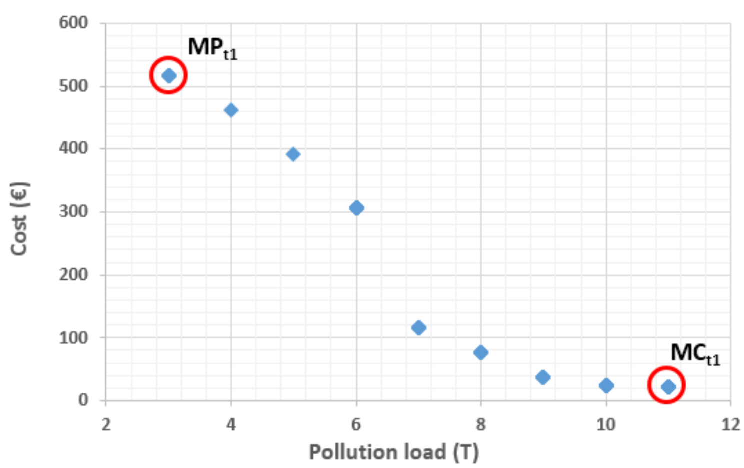

Figure 5 Pareto optimal front for 15 minutes

5.2 Solutions for the dynamic optimization process Based on the two extreme solutions in 0-15 minutes time-step, the dynamic optimization process was carried out for the minimum pollution load and minimum cost solutions for the total period of the storm (2 hours and 30 minutes). The Pareto optimal fronts obtained for minimum cost solution at different time-steps for the total storm period are exhibited in Figures 6a-i. As it was stated in the "Solution technique for the optimization problem" and "Real world application" sections, the control settings from a particular time-step for the minimum cost were used as the data to the next time-step optimization process. For example; control settings for MC_{t2} was used in finding the control settings for MC_{t3}.

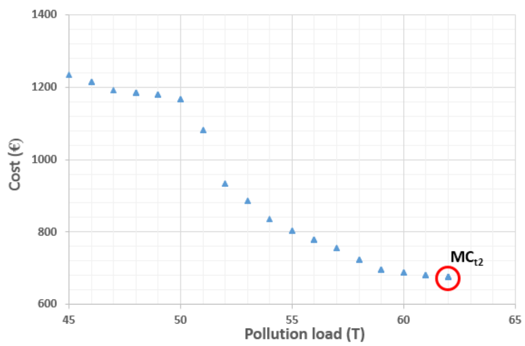

(a) For 15-30 minutes

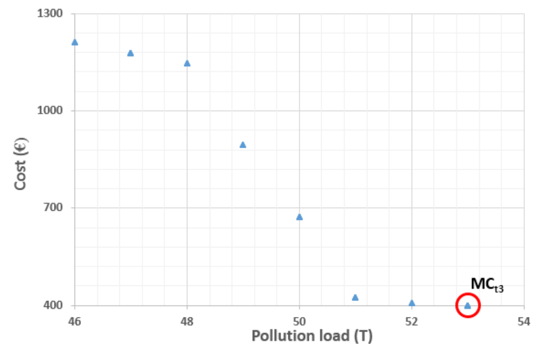

(b) For 30-45 minutes

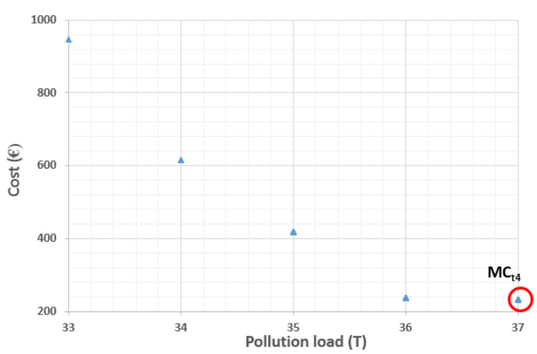

(c) For 45-60 minutes

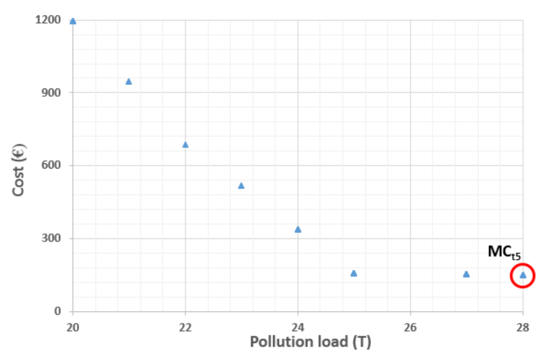

(d) For 60-75 minutes

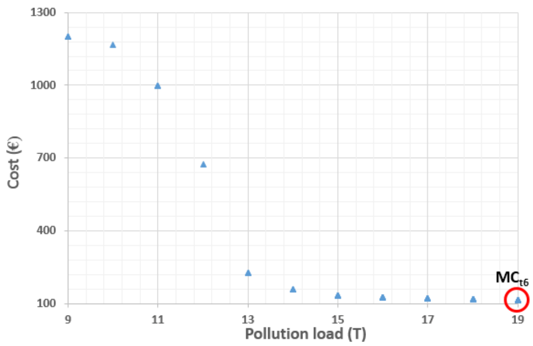

(e) For 75-90 minutes

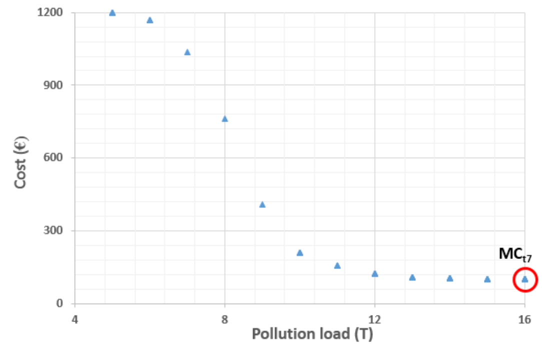

(f) For 90-105 minutes

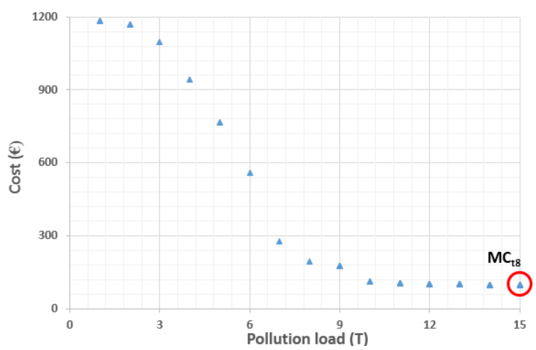

(g) For 105-120 minutes

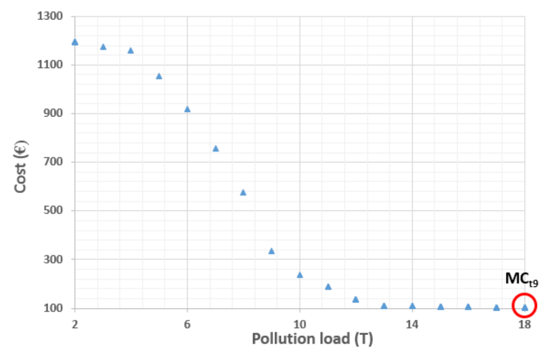

(h) For 120-135 minutes

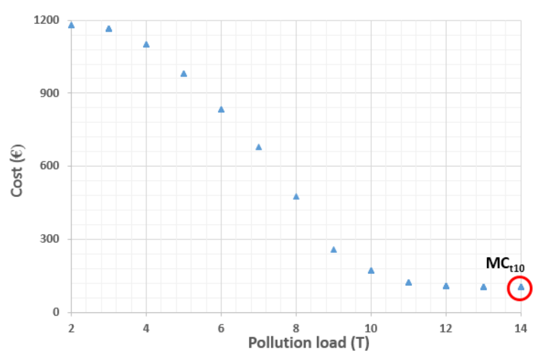

(i) For 135-150 minutes

Figure 6 Pareto optimal fronts for minimum cost solution over the time

All these Pareto fronts show the usual minimizing behavior or shape. In each time-step, the control settings for the minimum cost solution were extracted and then fed to the next time-step optimization process. Pareto optimal fronts over the time for the minimum pollution load solution are also similar to the Figures 6a-i (actual figure not shown). However, the Pareto optimal fronts show the minimizing behavior from their curved shapes (i.e. concave up with negative slopes).

5.3 Robustness of the optimization algorithm

The Figure 7a-b illustrate the Pareto optimal fronts for different initial seeds obtained for 15-30 minutes for minimum pollution load solution and at 105-120 minutes for minimum cost solution respectively. Each plot contains optimal fronts from 10 random runs with different initial populations in the genetic algorithm. They clearly show the coinciding effect of the optimal solutions from different initial seeds, but after 100 generations. Therefore, the Figures 7a-b clearly demonstrate the consistency and the stability of the developed genetic algorithm.

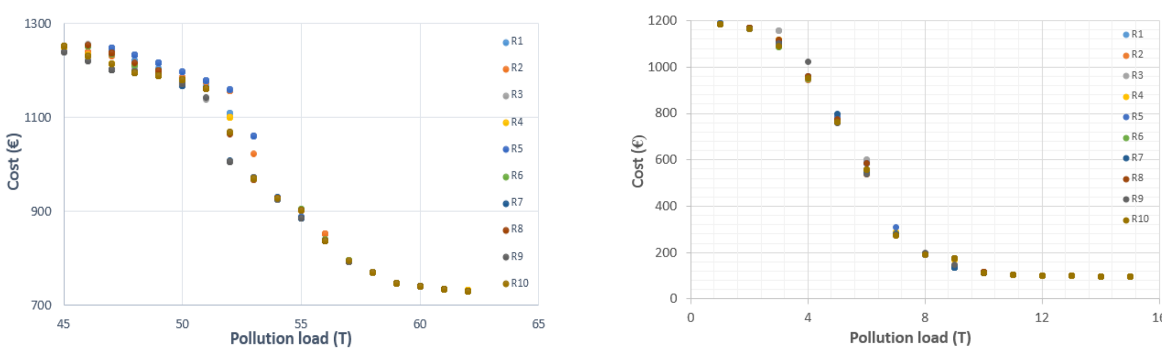

(a) At 30 minutes for minimum pollution load solution

(b) At 2 hours for minimum cost solution

Figure 7 Pareto optimal fronts for different initial seeds

The Figure 8 presents the progress of the genetic algorithm in optimal solution obtaining for the third time-step (30-45 minutes). As it can be expected in genetic algorithms in searching optimal solutions, Figure 8 illustrates a rapid convergence toward the minimum cost solution in 1000 function evaluations compared to the minimum cost in 100 function evaluations. However, after that, the cost solution converges to the minimum solution. Nevertheless, if the sewer controller is looking for a solution at a reasonable computational cost, he/she can stop the optimization process at 2000 function evaluations rather than completing 10000 function evaluations in the optimization process. This control possibility is given in Table 1.

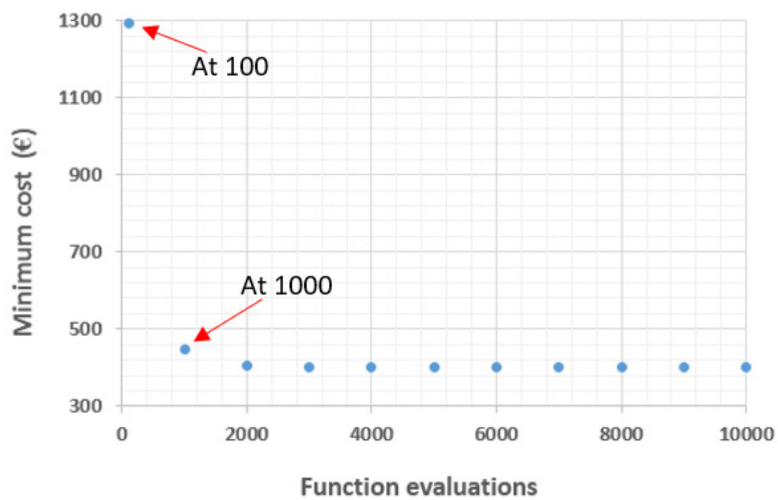

Figure 8 Progress of GA for minimum cost solution at T3

However, a similar but an interesting progressing behavior can be observed in minimum pollution load solutions. Unlike, the Figure 8, the process does not show a rapid convergence after the 100 function evaluations. Instead, it shows an increase of the pollution load solution. In fact, even the final optimal pollution load after 10000 function evaluations is numerically higher than the pollution load at 100 function evaluations. The circled solution was further investigated and found that it is an infeasible solution, which was generated initially in the process. Therefore, this solution can be ignored as we are only looking for the feasible solutions. After ignoring the first infeasible solution, the process shows the usual minimizing convergence. Therefore, the productivity of the developed genetic algorithm in achieving optimal results was achieved.

5.4 Comparison of solutions

Table 1 presents the comparison of solutions for 2000 and 10000 function evaluations for the solution presented in Figure 8. The table clearly shows the benefit of obtaining optimal solutions at the premature level of the process. For example, there is no significant difference in cost solutions for 3rd time step at 2000 and 10000 function evaluations (€404 and €400, respectively). In addition, their corresponding pollution loads are the same (53 T each). Similar observations can be seen for the other time steps as well as the solutions in minimum pollution load solutions.

Table 1 Comparison of solutions at 2000 and 10000 function evaluations

Minimum cost solution at 3rd time step		
	Cost (€)	Corresponding pollution load (T)
At 2000 function evaluations	404	53
At 10000 function evaluations	400	53

The results after the complete optimization process for the whole storm period revealed that the minimum pollution load solution has pollution load of **176 tons** for the total storm period (for 0-150 minutes). This pollution load is at a cost of **€11617**. However, the minimum cost solution has a cost of **€1997** over the total storm period at **273 tons** of pollution load. Therefore, the solutions satisfy the aim of the developed objective functions in the multi-objective optimization environment.

In addition, the most important finding of this optimization is the dynamic control of the sewer system for the two extreme solutions. In other words, it was found two sets of orifice openings for the minimum pollution load and minimum cost solution over the 150 minutes. The minimum pollution load solution has 7 orifice opening settings for O1- O7. Each orifice opening has a dynamic controlling behavior based on the developed novel optimization algorithm. This dynamic control behavior presents 10 steps of orifice openings for 0-150 minutes in 15 minute intervals. The similar control settings were found to the minimum cost solution. Therefore, each orifice has 10 control settings over the 150 minutes.

5.5 Optimal control gate openings

Some of the orifice settings obtained from the optimization process was illustrated in Figure 9. Figure 9a presents the orifice openings for minimum pollution load for O1 orifice. It clearly shows the dynamic behavior in each time-step. From 15 minutes to 15 minutes, the orifice opening changes. However, the opening heights were not from pre-defined step to step openings; instead the openings can be any height along real number axis from minimum opening to the maximum opening height. In other words, the opening heights are not in the binary axis where is has step responses, but in real number axis with any number of decimals. In comparison, Figure 9b presents orifice opening heights for O1 orifice for the minimum cost solution. Similar to the minimum pollution load solution case, Figure 9b also shows the dynamic behavior of the orifice heights over the 150 minutes. However, after the first 15 minutes, the orifice O1 is practically closed until 75 minutes and then slightly opened for 75-90 and 90-105 minutes. It is again closed for 30 minutes and opened for the 135-150 minutes. Therefore, in comparison to the O1 openings at Figure 9a, figure 9b shows reduced openings for minimum cost solution. Incidentally, this can be seen bit awkward situation and one would think the two figures have to be swapped for the titles of them. In other words, one would expect to have smaller openings of orifices and then to minimize the sewer overflows from the chamber for the minimum pollution load solution. Similarly, to have larger orifice openings in minimum cost solution which can lead more sewer overflows and then, to reduce the load at treatment plant to minimize the cost. However, it is well noted here that the objective function on pollution load is not totally based on the volumetric flow rate of combined sewer overflow, but it has many other water quality constituents' concentrations. Therefore, this justifies the novelty of the developed optimization algorithm from many other developed algorithms in the basis of volumetric minimization of combined sewer overflow.

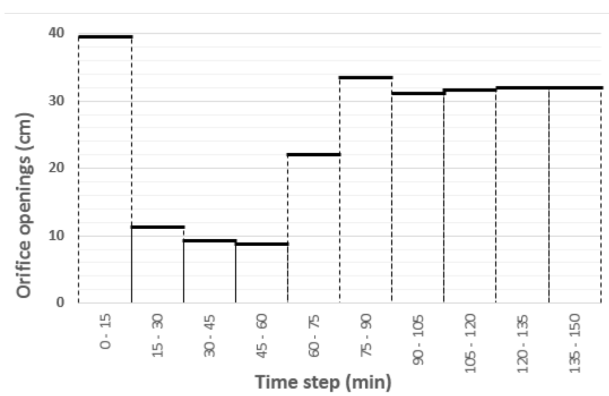

(a) Orifice openings for O1 for the minimum pollution load solution

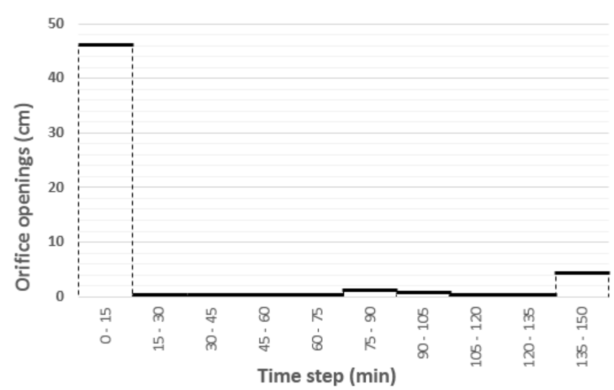

(b) Orifice openings for O1 for the minimum cost solution

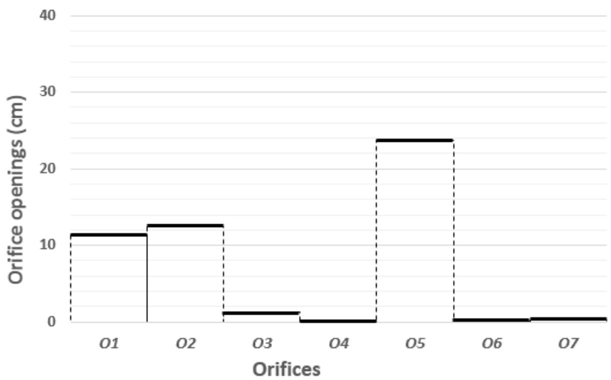

(c) Orifice openings for 15-30 minutes for the minimum pollution load solution

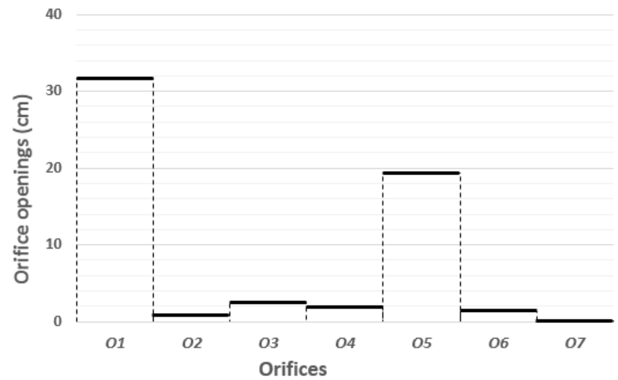

(d) Orifice openings for 120-135 minutes for the minimum pollution load solution

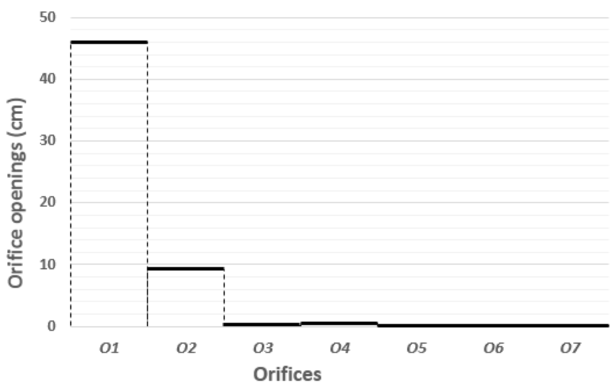

(e) Orifice openings for 15-30 minutes for the minimum cost solution

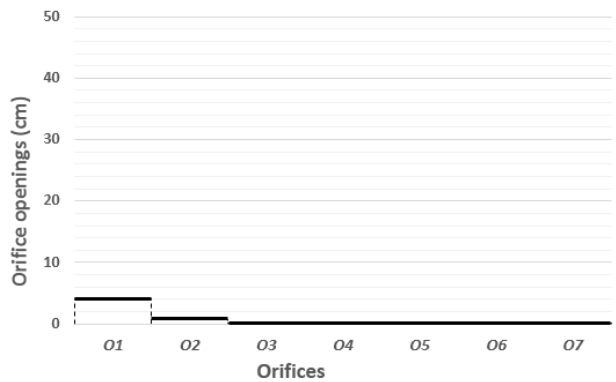

(f) Orifice openings for 135-150 minutes for the minimum pollution load solution

Figure 9 Orifice openings for some of the orifices

Figures 9c and 9d present the orifice openings for 15-30 minutes time step and 120-135 minutes time step for the minimum pollution load solution. The figures clearly show the different control settings (orifice openings) for different orifices (O1 to O7). Therefore, it gives the applicability of the developed algorithm in spatial variation of control settings. In addition, the two figures at different time-steps guarantee the temporal variations of the control settings. Similarly, Figures

9e and 9f illustrate the orifice openings for 15-30 minutes time step and 135-150 minutes time step for the minimum cost solution. Orifice openings for the same time-step; however, for the two different extreme solutions are given in figures 9c and 9e. They clearly exhibit the applicability of the developed algorithm in different approaches. Therefore, the orifice openings (control settings) can be obtained depending on the desire of the sewer network controller. If the cost is more important, the controller can go for a cost prioritizing solution, whereas, if the pollution load is more important, the controller can look at a solution, which priorities the pollution load. The most important feature is that the controller can even look into these solutions at a smaller time step (even at 15 minutes). In addition, these four Figures 9c-f clearly show the spatial and temporal features of the control algorithm.

5.6 Hydraulic analysis of selected solutions

The Figure 10 presents the flow through sewer conduits for the total storm period for the minimum pollution load solution. These flow rates were obtained from the hydraulic simulations by feeding the control settings found from the optimization analysis. The dashed line on top of each figure (Figures 10a-g) gives the maximum possible flow rate allowed through the sewer conduits. These flow rates were imposed to the control algorithm as the constraints. The figures clearly show that none of the sewer conduits have flow rates more than the allowed flow rates. Those justify the constraint handling ability of the developed algorithm. In addition, they show the temporal variation of the flow rates through sewer conduits. However, the flow rates through sewer conduits are lowered from the controlling algorithm to keep the minimum cost solution. A significant component of the cost function depends on the treated wastewater volume. Therefore, in the minimum cost solution, the algorithm tries to reduce the flow rate to the sewer treatment plant, thus to reduce the treatment cost. However, in contrast, the flow rates through the conduits for minimum pollution load solution have to be higher than the flow rates shown in Figure 10. More flows are allowed through the conduits to minimize the pollution loads from the CSOs. This observation can be seen in the hydraulic simulated results for the minimum pollution load solution.

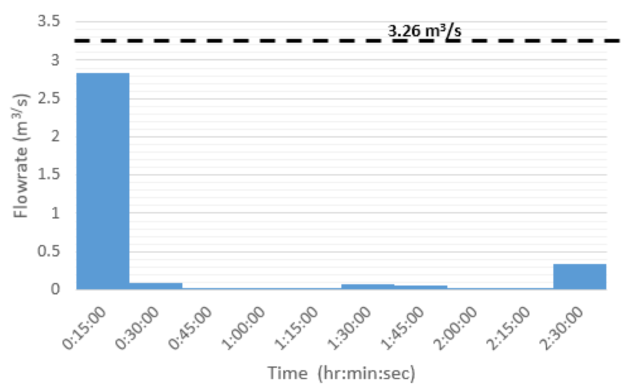

(a) Flow through *C1*

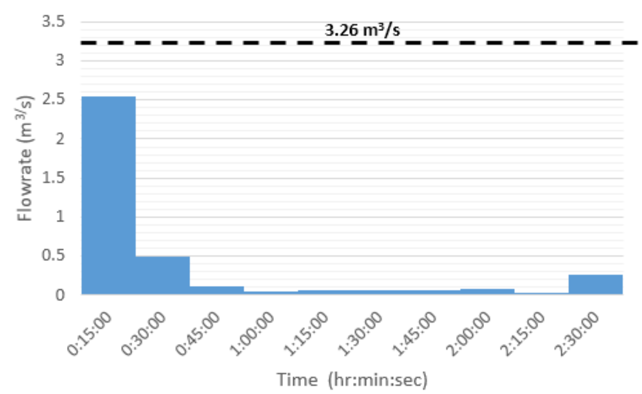

(b) Flow through *C2*

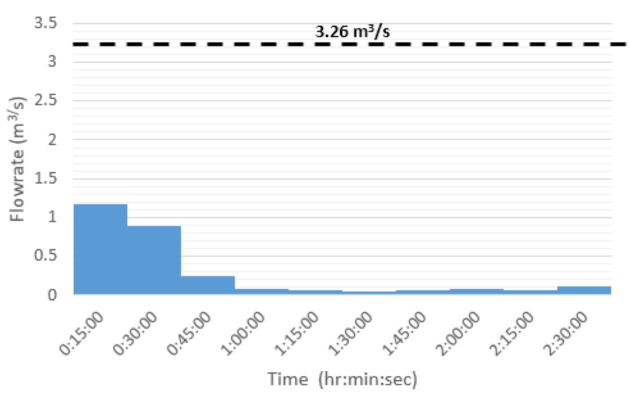

(c) Flow through *C3*

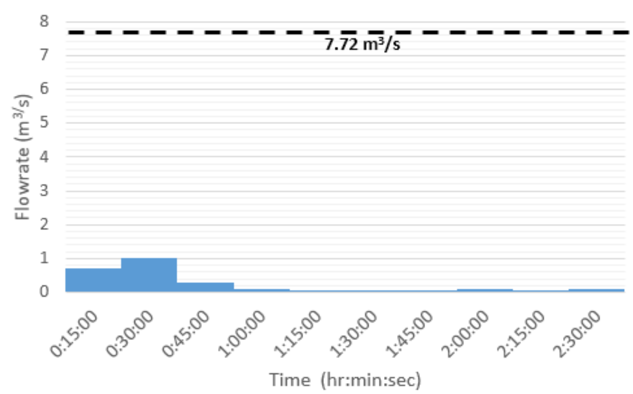

(d) Flow through *C4*

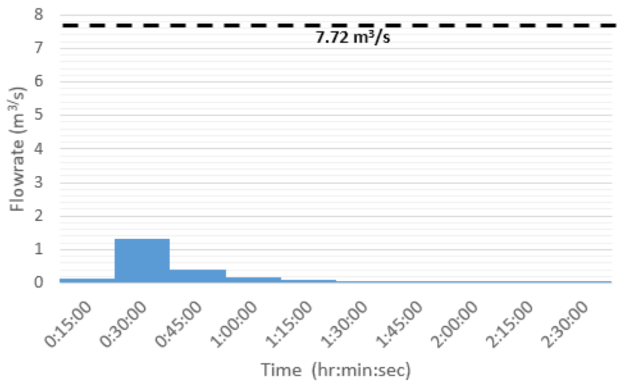

(e) Flow through *C5*

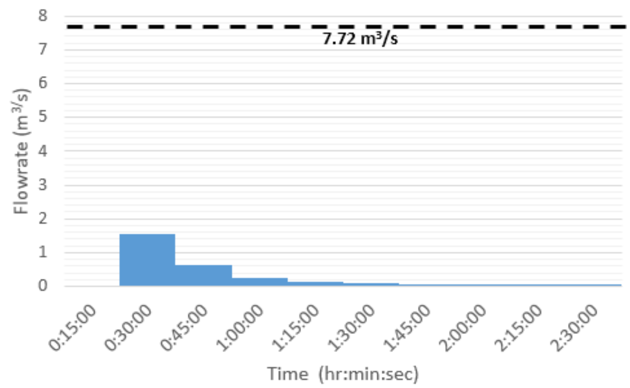

(f) Flow through *C6*

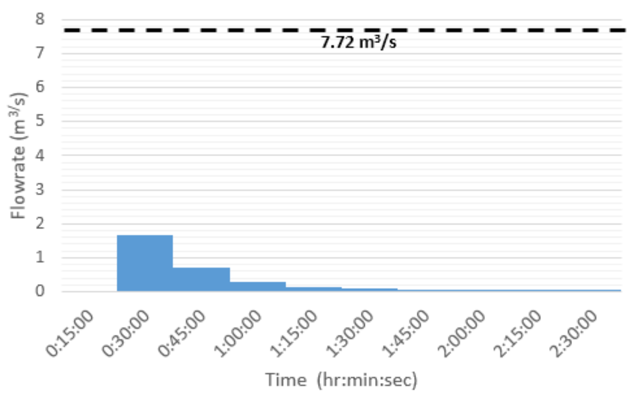

(g) Flow through *C7*

Figure 10 Flow rates through sewer conduits for minimum cost solution

Figures 11a illustrates the wastewater heights in the T1 sewer chamber for the minimum cost solution. The dashed line shows the maximum height, which the sewer chamber can hold before any CSOs. Therefore, the wastewater heights more than the dashed lines, reflect the CSOs. These sewer chambers acting as another storage tanks (on-line); however, they are with the possibility of having CSOs. The hydraulic importance of having the storage tanks were discussed earlier; nevertheless, they keep a reasonable sewer volume without releasing as CSOs. Therefore, the optimization algorithm tries to have some overflows depending on the volumes or capacities of the sewer chambers. Figure 11b presents the wastewater heights in one of the on-line storage tanks. Similar to the sewer chambers, the dashed lines represent the maximum heights of the storage tank. However, unlike the sewer chambers, the wastewater heights are not exceeding the maximum heights of the storage tanks. Therefore, the algorithm has the ability to keep the role of the storage tanks, i.e. with no CSOs. Even though the storage tanks do not have any CSOs, they are completely filled by the wastewater for the total time. Therefore, the stored wastewater can be released back to the sewer system after the storm.

Nevertheless, Figure 11c illustrates the wastewater heights in the off-line storage tank. This off-line tank works with a hydraulic pump. Interestingly, the storage tank is not completely filled similar to the other two on-line storage tanks. This is because the implementations of new cost function, which includes the cost of pump operation. As it was stated earlier, pump operational cost is a function of the pumped wastewater volume flow rate. Therefore, to minimize pump operational cost, the algorithm minimizes the pumped volume flow rate. Instead, the control algorithm allows to transfer the wastewater to the on-line storage tanks. Similar results can be seen in the minimum pollution load solution wastewater heights. Thus the results clearly revealed that the roles of sewer chambers, on-line storage tanks and off-line storage tanks with improved cost objective functions are satisfied.

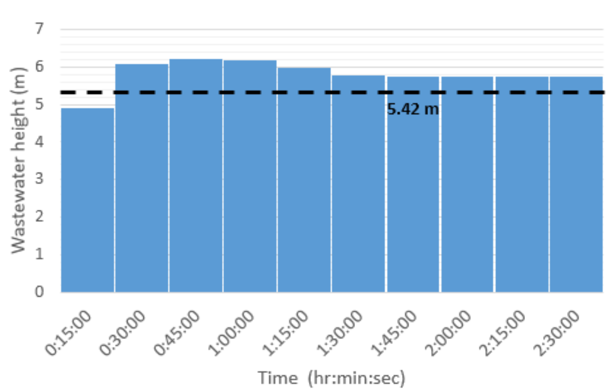

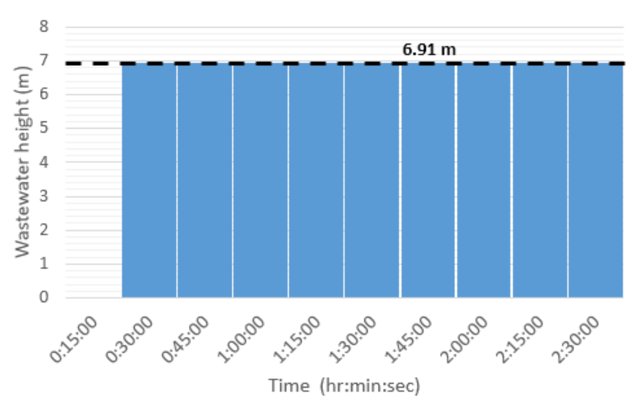

(a) Wastewater height of T1

(b) Wastewater height of T8

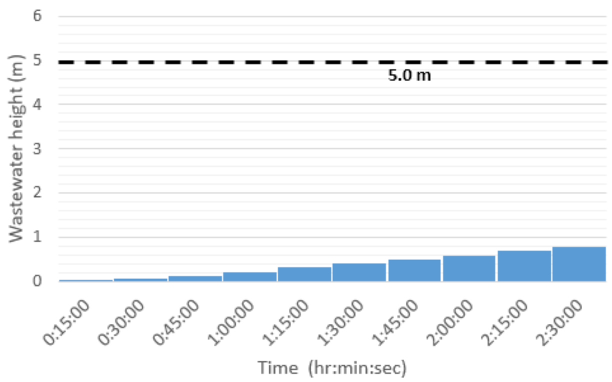

(c) Wastewater height of T10

Figures 11 wastewater heights in the sewer chambers and storage tanks for the minimum cost solution

The control algorithm developed in this study is unique as it can simultaneously minimize two of the most important objectives i.e., pollution load to receiving water from CSOs and the total wastewater treatment and pumping cost of the system. The presented algorithm is the first attempt capable of handling the simultaneous solutions of the multiple objectives and processing the control settings varied in temporal and spatial domains. Unlike most of the other real time optimal controls, this approach finds the hydraulic, hydrological and water quality solutions from full hydraulic simulations. Though this method was applied to an existing network in Liverpool, UK but the optimization algorithm is generic and can be applied anywhere.

6. Conclusions

A novel algorithm based on multi-objective optimization is presented here to control the combined sewer networks. The algorithm is capable of minimizing the pollution load to the receiving water from the CSOs together with the cost of wastewater treatment and pumping cost in sewer system. The algorithm produces temporally and spatially varied dynamic control settings of the gates in sewer system. These control settings can be obtained as per the requirements of the authorities of the combined sewer system depending on the available financial situation and environmental regulations of the country. Usage of storage tanks in combined sewer systems was justified in the optimal solutions as the algorithm allows the storage tanks to be completely utilized. However, when it comes to incorporate a pump, which adds an operation and maintenance cost that particular storage tank was discouraged by the algorithm. Therefore, the introduced objective functions to the algorithm are satisfying the requirement of the authorities as well as the generic public.

Even though the algorithm produces dynamic control settings based on the feedbacks given to the system, the solution algorithm is yet to be applied in the real-time. This is due to the computational cost of the algorithm. The algorithm needs to be improved in simulation times, so that it can be applied real-time. However, the developed control algorithm is well-structured to deal with the receiving water qualities and the cost incurred in the wastewater systems. The approach provides a holistic solution as it incorporates the spatial and temporal variations of flows and pollution concentrations in addition to the non-simplified hydraulic and water quality modeling in combined sewer network. Furthermore, the input parameters for the cost function can be easily improved depending on the economic status of a particular country or concerned area. Therefore, the algorithm would make a greater change in the related applications.

References

1. Abo-Sinna, M., Baky, I., 2007. Interactive balance space approach for solving multi-level multi-objective programming problems. Information Sciences. 177, 3397-3410.
2. Aghaei, J., Amjady, N., Shayanfar, H., 2011. Multi-objective electricity market clearing considering dynamic security by lexicographic optimization and augmented epsilon constraint method. Applied Soft Computing. 11, pp. 3846-3858.
3. Alizadeh, M., Nikoo, M., Rakhshandehroo, G., 2017. Hydro-environmental management of groundwater resources: A fuzzy-based multi-objective compromise approach. Journal of Hydrology. 551, pp. 540-554.
4. Anne-Sophie, M., Dorner, S., Sauvé, S., Aboulfadl, K., Galarneau, M., Servais, P., Prévost, M., 2015. Temporal analysis of E. coli, TSS and wastewater micropollutant loads from combined sewer overflows: implications for management. Environmental Science: Processes & Impacts. 17, pp. 965-974.
5. Bekele, E., Nicklow, J., 2007. Multi-objective automatic calibration of SWAT using NSGA-II. Journal of Hydrology. 341, pp. 165-176.
6. Benedetti L., Bixio D. Vanrolleghem P.A. 2006. Benchmarking of WWTP design by assessing costs, effluent quality and process variability. Water Science and Technolog. 54(10), pp. 95-102
7. Berndtsson, R., Niemczynowicz, J., 1988. Spatial and temporal scales in rainfall analysis — Some aspects and future perspectives. Journal of Hydrology. 100, pp. 293-313.
8. Brokamp, C., Beck, A., Muglia, L., Ryan, P., 2017. Combined sewer overflow events and childhood emergency department visits: A case-crossover study. Science of The Total Environment. 607-608, pp. 1180-1187.

9. Brunetti, G., Šimůnek, J., Piro, P., 2016. A comprehensive numerical analysis of the hydraulic behavior of a permeable pavement. Journal of Hydrology. 540, pp. 1146-1161.
10. Brzezińska, A., Zawilski, M. Sakson, G. 2016. Assessment of pollutant load emission from combined sewer overflows based on the online monitoring. Environmental Monitoring and Assessment, 188(9), pp.502-511.
11. Carpinelli, G., Caramia, P., Mottola, F., Proto, D., 2014. Exponential weighted method and a compromise programming method for multi-objective operation of plug-in vehicle aggregators in microgrids. International Journal of Electrical Power & Energy Systems. 56, pp. 374-384.
12. Chang, L., Chang, F., 2009. Multi-objective evolutionary algorithm for operating parallel reservoir system. Journal of Hydrology. 377, pp. 12-20.
13. Charnes, A., Cooper, W., 1977. Goal programming and multiple objective optimizations. European Journal of Operational Research. 1, pp. 39-54.
14. Chen, J., Liu, Y., Gitau, M., Engel, B., Flanagan, D., Harbor, J., 2019. Evaluation of the effectiveness of green infrastructure on hydrology and water quality in a combined sewer overflow community. Science of The Total Environment. 665, pp. 69-79.
15. Congcong, S., Joseph-Duran, B., Maruejouls, T., Cembrano, G., Meseguer, J., Puig, V. and Litrico, X. 2019. Real-Time Control-Oriented Quality Modelling in Combined Urban Drainage Networks. In: *The 20th World Congress of the International Federation of Automatic Control*. Toulouse, France.
16. Costa, N., Lourenço, J., Pereira, Z. 2011. Multiresponse Optimization and Pareto Frontiers. Quality and Reliability Engineering International. 28(7), pp.701-712.
17. Davis, L., 1991. Handbook of genetic algorithms. Van Nostrand Reinhold, New York.

18. Deb, K., Pratap, A., Agarwal, S. and Meyarivan, T. 2002. A fast and elitist multiobjective genetic algorithm: NSGA-II. IEEE Transactions on Evolutionary Computation. 6(2), pp.182-197.

19. Dirckx, G., Korving, H., Bessembinder, J., Weemaes, M., 2017. How climate proof is real-time control with regard to combined sewer overflows?. Urban Water Journal. 15, pp. 544-551.

20. Entem, S., Lahoud, A., Yde, L., Bendsen, B., 1998. Real time control of the sewer system of boulogne billancourt - a contribution to improving the water quality of the seine. Water Science and Technology. 37, pp. 327-332.

21. Erbe, V., Risholt, L., Schilling, W., Londong, J. 2002. Integrated modelling for analysis and optimisation of wastewater systems–the Odenthal case. Urban Water Journal, 4(1), pp. 63–71.

22. Fu, X., Goddard, H., Wang, X., Hopton, M., 2019. Development of a scenario-based stormwater management planning support system for reducing combined sewer overflows (CSOs). Journal of Environmental Management. 236, pp. 571-580.

23. García, J., Espín-Leal, P., Vigueras-Rodriguez, A., Castillo, L., Carrillo, J., Martínez-Solano, P., Nevado-Santos, S. 2017. Urban Runoff Characteristics in Combined Sewer Overflows (CSOs): Analysis of Storm Events in Southeastern Spain. Water. 9(5), pp. 303-318.

24. Gasperi, J., Zgheib, S., Cladière, M., Rocher, V., Moilleron, R. and Chebbo, G. 2012. Priority pollutants in urban stormwater: Part 2 – Case of combined sewers. Water Research. 46(20), pp. 6693-6703.

25. Georgaki, S., Vernon, D., Baur, R., Black, D. and Crawford, D. 2018. Extended CSO control storage: what could possibly go wrong?. Water Practice and Technology. 13(1), pp.184-190.

26. Grefenstette, J., 1986. Optimization of Control Parameters for Genetic Algorithms. IEEE Transactions on Systems, Man, and Cybernetics. 16, pp. 122-128.

27. Hermoso, M., García-Ruiz, M., Osorio, F. 2018. Efficiency of Flood Control Measures in a Sewer System Located in the Mediterranean Basin. Water. 10(10), pp.1437-1450.

28. Hofer, T., Montserrat, A., Gruber, G., Gamerith, V., Corominas L., Muschalla, D. 2018. A robust and accurate surrogate method for monitoring the frequency and duration of combined sewer overflows. Environmental Monitoring and Assessment. 190(4), pp. 209-226.

29. Hu, C., Teng, C., Li, S., 2007. A fuzzy goal programming approach to multi-objective optimization problem with priorities. European Journal of Operational Research. 176, pp. 1319-1333.

30. Jalliffier-Verne, I., Heniche, M., Madoux-Humery, A., Galarneau, M., Servais, P., Prévost, M., Dorner, S., 2016. Cumulative effects of fecal contamination from combined sewer overflows: Management for source water protection. Journal of Environmental Management. 174, pp. 62-70.

31. Jean, M., Duchesne, S., Pelletier, G., Pleau, M., 2018. Selection of rainfall information as input data for the design of combined sewer overflow solutions. Journal of Hydrology. 565, pp. 559-569.

32. Jee, K., McShan, D., Fraass, B., 2007. Lexicographic ordering: intuitive multicriteria optimization for IMRT. Physics in Medicine and Biology. 52, pp. 1845-1861.

33. Joseph-Duran, B., Ocampo-Martinez, C., Cembrano, G., 2015. Output-feedback control of combined sewer networks through receding horizon control with moving horizon estimation. Water Resources Research. 51, pp. 8129-8145.

34. Kang, N., Kokkolaras, M., Papalambros, P., 2014. Solving multiobjective optimization problems using quasi-separable MDO formulations and analytical target cascading. Structural and Multidisciplinary Optimization. 50, pp. 849-859.

35. Kim, I., de Weck, O., 2004. Adaptive weighted-sum method for bi-objective optimization: Pareto front generation. Structural and Multidisciplinary Optimization. 29, pp. 149-158.

36. Kim, M., Rao, S., Yoo C. 2009. Dual optimization strategy for N and P removal in a biological wastewater treatment plant. Industrial and Engineering Chemistry Research. 48: pp. 6363-6371.

37. Lei, X., Zhang, J., Wang, H., Wang, M., Khu, S., Li, Z., Tan, Q., 2018. Deriving mixed reservoir operating rules for flood control based on weighted non-dominated sorting genetic algorithm II. Journal of Hydrology 564. Pp. 967-983.

38. Leisenring, M., Moradkhani, H., 2012. Analyzing the uncertainty of suspended sediment load prediction using sequential data assimilation. Journal of Hydrology. 468-469, pp. 268-282.

39. Lucas, W., Sample, D., 2015. Reducing combined sewer overflows by using outlet controls for Green Stormwater Infrastructure: Case study in Richmond, Virginia. Journal of Hydrology. 520, pp. 473-488.

40. Madoux-Humery, A., Dorner, S., Sauvé, S., Aboulfadl, K., Galarneau, M., Servais, P., Prévost, M., 2016. The effects of combined sewer overflow events on riverine sources of drinking water. Water Research. 92, pp. 218-227.
41. Mahmoodian, M., Delmont, O., Schutz, G. 2017. Pollution-based model predictive control of combined sewer networks, considering uncertainty propagation. International Journal of Sustainable Development and Planning. 12(01), pp.98-111.
42. Maneta, M., Pasternack, G., Wallender, W., Jetten, V., Schnabel, S., 2007. Temporal instability of parameters in an event-based distributed hydrologic model applied to a small semiarid catchment. Journal of Hydrology. 341, pp. 207-221.
43. Marler, R., Arora, J., 2004. Survey of multi-objective optimization methods for engineering. Structural and Multidisciplinary Optimization. 26, pp. 369-395.
44. Marler, R., Arora, J., 2009. The weighted sum method for multi-objective optimization: new insights. Structural and Multidisciplinary Optimization. 41, pp. 853-862.
45. Mauricio-Iglesias, M., Montero-Castro, I., Mollerup, A., Sin, G., 2015. A generic methodology for the optimisation of sewer systems using stochastic programming and self-optimizing control. Journal of Environmental Management. 155, pp. 193-203.
46. Meneses, E., Gaussens, M., Jakobsen, C., Mikkelsen, P., Grum, M., Vezzaro, L. 2018. Coordinating Rule-Based and System-Wide Model Predictive Control Strategies to Reduce Storage Expansion of Combined Urban Drainage Systems: The Case Study of Lundtofte, Denmark. Water. 10(1), pp.76-90.
47. Morales, V., 2016. Urban drainage modeling and evolutionary multiobjective optimization for combined sewer overflows prediction and control, PhD thesis. University of Illinois at Urbana-Champaign, United States.

48. Morales, V., Mier, J., Garcia, M., 2015. Innovative modeling framework for combined sewer overflows prediction. Urban Water Journal. 14, pp. 97-111.

49. Müller, T., Schütze, M., Bárdossy, A., 2017. Temporal asymmetry in precipitation time series and its influence on flow simulations in combined sewer systems. Advances in Water Resources. 107, pp. 56-64.

50. Naserizade, S., Nikoo, M., Montaseri, H., 2018. A risk-based multi-objective model for optimal placement of sensors in water distribution system. Journal of Hydrology. 557, pp. 147-159.

51. Nasri, V., Haynes, C., 2015. New tunnel system to eliminate sanitary sewer overflows and control combined sewer overflows in Hartford, Connecticut. Water Practice & Technology. 10, pp. 282-290.

52. Nie, L., Lindholm, O., Lindholm, G., Syversen, E. 2009. Impacts of climate change on urban drainage systems—A case study in Fredrikstad, Norway. Urban Water Journal. 6, pp. 323–332.

53. Ogidan, O., Giacomoni, M., 2016. Multiobjective Genetic Optimization Approach to Identify Pipe Segment Replacements and Inline Storages to Reduce Sanitary Sewer Overflows. Water Resources Management. 30, pp. 3707-3722.

54. Pennino, M., McDonald, R., Jaffe, P., 2016. Watershed-scale impacts of stormwater green infrastructure on hydrology, nutrient fluxes, and combined sewer overflows in the mid-Atlantic region. Science of The Total Environment. 565, pp. 1044-1053.

55. Qiu, H., Dong, Y., Wang, Y., Gao, L., 2011. Tolerance Optimization Design Based on Physical Programming Methods and PSO Algorithm. Advanced Materials Research. 346, pp. 584-592.

56. Rathnayake, U., Tanyimboh, T. 2015. Evolutionary Multi-Objective Optimal Control of Combined Sewer Overflows. Water Resources Management. 29(8), pp.2715-2731.
57. Rathnayake, U.S., 2013. Optimal management and operational control of urban sewer systems, PhD thesis. University of Strathclyde, Glasgow, United Kingdom.
58. Rathnayke U.S. (2018) Static optimal control of combined sewer networks under enhanced cost functions to minimize the adverse environmental effects. ISH Journal of Hydraulic Engineering. doi.org/10.1080/09715010.2018.1541765
59. Read G.F. 2004. Sewers replacement and new construction. Elsevier ltd. 1st edition. ISBN 0 7506 5083 4. pp. 77
60. Read G.F., Vickridge I. 1997. Sewers rehabilitation and new construction, repair and renovation. Elsevier ltd. 1st edition. ISBN 0 340 54472 4. pp. 314
61. Rodriguez, F., Andrieu, H., Creutin, J., 2003. Surface runoff in urban catchments: morphological identification of unit hydrographs from urban databanks. Journal of Hydrology. 283, pp. 146-168.
62. Rossman L.A. 2009. US EPA SWMM 5.0 User's Manual EPA/600/R-05/040, Water Supply and Water Resources Division, National Risk Management Research Laboratory, Cincinnati, USA.
63. Ryu, J., Baek, H., Lee, G., Kim, T., Oh, J., 2015. Optimal planning of decentralised storage tanks to reduce combined sewer overflow spills using particle swarm optimisation. Urban Water Journal. 14, pp. 202-211.
64. Saagi, R., Flores-Alsina, X., Fu, G., Butler, D., Gernaey, K., Jeppsson, U. 2016. Catchment & sewer network simulation model to benchmark control strategies within urban wastewater systems. Environmental Modelling & Software. 78, pp.16-30.

65. Saagi, R., Kroll, S., Flores-Alsina, X., Gernaey, K., Jeppsson, U. 2018. Key control handles in integrated urban wastewater systems for improving receiving water quality. Urban Water Journal. 15(8), pp.790-800.

66. Schertzinger, G., Zimmermann, S., Sures, B., 2019. Predicted sediment toxicity downstream of combined sewer overflows corresponds with effects measured in two sediment contact bioassays. Environmental Pollution. 248, pp. 782-791.

67. Seggelke, K., Löwe, R., Beeneken, T., Fuchs, L. 2013. Implementation of an integrated real-time control system of sewer system and wastewater treatment plant in the city of Wilhelmshaven. Urban Water Journal, 10(5), pp.330-341.

68. Shimoda, M., Azegami, H., Sakurai, T., 1996. Multiobjective Shape Optimization of Linear Elastic Structures Considering Multiple Loading Conditions: Dealing with Mean Compliance Minimization problems. JSME international journal. Ser. A, Mechanics and material engineering. 39, pp. 407-414.

69. Singh, N., 2002. Integrated product and process design: a multi-objective modeling framework. Robotics and Computer-Integrated Manufacturing. 18, pp. 157-168.

70. Snodgrass, W., Dewey, R., D’Andrea, M., Bishop, R., Lei, J., 2018. Forecasting receiving water response to alternative control levels for combined sewer overflows discharging to Toronto’s Inner Harbour. Aquatic Ecosystem Health & Management. 21, pp. 245-254.

71. Soriano, L., Rubió, J., 2019. Impacts of Combined Sewer Overflows on surface water bodies. The case study of the Ebro River in Zaragoza city. Journal of Cleaner Production. 226, pp. 1-5.

72. Sørup, H., Lerer, S., Arnbjerg-Nielsen, K., Mikkelsen, P., Rygaard, M., 2016. Efficiency of stormwater control measures for combined sewer retrofitting under varying rain conditions: Quantifying the Three Points Approach (3PA). Environmental Science & Policy. 63, pp. 19-26.

73. Srinivas, N., Deb, K., 1994. Muiltiobjective Optimization Using Nondominated Sorting in Genetic Algorithms. Evolutionary Computation. 2, pp. 221-248.

74. Sun, C., Ritchie, S., Tsai, K., Jayakrishnan, R., 1999. Use of vehicle signature analysis and lexicographic optimization for vehicle reidentification on freeways. Transportation Research Part C: Emerging Technologies. 7, pp. 167-185.

75. Talebi, L., Pitt, R. 2019. Water Sensitive Urban Design Approaches in Sewer System Overflow Management. In: A. Sharma, T. Gardner and D. Begbie, ed., *Approaches to Water Sensitive Urban Design Potential, Design, Ecological Health, Urban Greening, Economics, Policies, and Community Perceptions*, 1st ed. Amsterdam, Netherlands: Elsevier Publishing Company, pp.140-161.

76. Tao, J., Li, Z., Peng, X., Ying, G. 2017. Quantitative analysis of impact of green stormwater infrastructures on combined sewer overflow control and urban flooding control. Frontiers of Environmental Science & Engineering. 11(4), pp.11-22.

77. Tavakol-Davani, H., Burian, S., Devkota, J., Apul, D. 2016b. Performance and Cost-Based Comparison of Green and Gray Infrastructure to Control Combined Sewer Overflows. Journal of Sustainable Water in the Built Environment. 2(2), pp.04015009-1 - 04015009-12.

78. Tavakol-Davani, H., Goharian, E., Hansen, C., Tavakol-Davani, H., Apul, D., Burian, S. 2016a. How does climate change affect combined sewer overflow in a system benefiting from rainwater harvesting systems? Sustainable Cities and Society. 27, pp.430-438.
79. Thomas N. 2000. Optimal pollution control models for interceptor sewer systems. PhD Thesis, University of Liverpool, UK.
80. Thomas N., Templeman A., Burrows R. 1999. Optimal pollution control models for interceptor sewers and overflow chambers. International Conference on Computing and Control for the Water Industry. Exeter, UK, pp. 265–278.
81. Thomas N., Templeman A., Burrows R. 2000. Pollutant load overspill minimization of interceptor sewer systems. Engineering Optimization. 32, pp. 393–416.
82. Vezzaro, L., Christensen, M., Thirsing, C., Grum, M. and Mikkelsen, P. 2014. Water Quality-based Real Time Control of Integrated Urban Drainage Systems: A Preliminary Study from Copenhagen, Denmark. Procedia Engineering, 70, pp.1707-1716.
83. Wang, F., Yeh, C., Wu, Y., 1996. PID controller tuning by an interactive multi-objective optimisation method. Transactions of the Institute of Measurement and Control. 18, pp. 183-192.
84. Wang, J., Guo, Y. 2018. An Analytical Stochastic Approach for Evaluating the Performance of Combined Sewer Overflow Tanks. Water Resources Research. 54(5), pp.3357-3375.
85. Wang, M., Liu, S., Wang, S., Lai, K., 2010. A weighted product method for bidding strategies in multi-attribute auctions. Journal of Systems Science and Complexity. 23, pp. 194-208.

86. Wang, R., Zhou, Z., Ishibuchi, H., Liao, T., Zhang, T., 2018. Localized Weighted Sum Method for Many-Objective Optimization. IEEE Transactions on Evolutionary Computation. 22, pp. 3-18.
87. Wei, Z., Huang, X., Lu, L., Shangguan, H., Chen, Z., Zhan, J., Fan, G. 2019. Strategy of Rainwater Discharge in Combined Sewage Intercepting Manhole Based on Water Quality Control. Water. 11(5), pp.898-911.
88. Weinreich, G., Schilling, W., Birkely, A. and Moland, T. (1997). Pollution based real time control strategies for combined sewer systems. Water Science and Technology, 36(8-9), pp.331-336.
89. Yuan, Y., Ling, Z., Gao, C., Cao, J., 2014. Formulation and application of weight-function-based physical programming. Engineering Optimization. 46, pp. 1628-1650.
90. Zhang, D., Lindholm, G., Ratnaweera, H. 2018b. Use long short-term memory to enhance Internet of Things for combined sewer overflow monitoring. Journal of Hydrology. 556, pp.409-418.
91. Zhang, D., Martinez, N., Lindholm, G., Ratnaweera, H. 2018a. Manage Sewer In-Line Storage Control Using Hydraulic Model and Recurrent Neural Network. Water Resources Management. 32(6), pp.2079-2098.
92. Zhang, W., Shivpuri, R., 2009. Probabilistic design of aluminum sheet drawing for reduced risk of wrinkling and fracture. Reliability Engineering & System Safety. 94, pp. 152-161.
93. Zhao, J., Psychoudakis, D., Chen, C., Volakis, J. 2012. Design Optimization of a Low-Profile UWB Body-of-Revolution Monopole Antenna. IEEE Transactions on Antennas and Propagation. 60(12), pp.5578-5586.

94. Zhao, W., Beach, T., Rezgui, Y. 2017. Automated Model Construction for Combined Sewer Overflow Prediction Based on Efficient LASSO Algorithm. IEEE Transactions on Systems, Man, and Cybernetics: Systems. pp.1-16.

95. Zheng, G., Bi, Q., Zhu, L., 2011. Smooth tool path generation for five-axis flank milling using multi-objective programming. Proceedings of the Institution of Mechanical Engineers, Part B: Journal of Engineering Manufacture. 226, pp. 247-254.

96. Zimmer, A., Schmidt, A., Ostfeld, A., Minsker, B. 2015. Evolutionary algorithm enhancement for model predictive control and real-time decision support. Environmental Modelling & Software. 69, pp.330-341.

97. Zimmer, A., Schmidt, A., Ostfeld, A., Minsker, B. 2018. Reducing Combined Sewer Overflows through Model Predictive Control and Capital Investment. Journal of Water Resources Planning and Management. 144(2), pp.04017091-1 - 04017091-11.